



3D NON-LINEAR DYNAMIC RESPONSE OF ROCK FILL DAM USING MOHR-COULOMB YIELDING CRITERIA

Violeta MIRCEVSKA¹ and Vladimir BICKOVSKI²

SUMMARY

A computer programme for three-dimensional non-linear static and seismic analysis incorporating the Mohr criteria of non-linear behaviour of friction materials has been elaborated. The non-linear analysis gives us the possibility to define, i.e., detect zones in which excessive tensile stresses and occurrence of cracks are expected. Definition of effective stresses and effective stiffness characteristics is necessary. For that purpose, a computer programme has been elaborated to analyse the filtration flows through 3D porous coherent material media under the conditions of a stationary filtration regime, as a most common phase of dam serviceability. In the contact zone foundation-dam contact elements of linear type are placed. A three-dimensional discrete mathematical model created by substructures and discrete network of isoparametric finite elements with 8 and 6 nodal points is used. A computer programme for automatic generation of 3D geometry of the dam body has been elaborated based on the topology of the terrain.

The results from such an analysis enable detection of zones prone to cracks particularly in the clayey core during strong earthquakes. The non-linear treatment of rock-fill dams enables determination of the plastic deformations of the dam after earthquakes. Based on these deformations and the defined time histories of the safety coefficient against sliding of some potential sliding surfaces, an engineering judgement about the stability of the dam under a certain seismic level of acceleration can be made. Using computer visualization of the dam response, we are able to follow the evaluation of stresses and appearance of cracks during excitation.

AUTOMATIC GENERATION OF 3D MATHEMATICAL MODEL

Automatic generation of 3D mathematical models required the database on topology of the terrain, position of the axis of the dam crest at the base, fig. 1, and the shape of the characteristic central cross-section of the dam, fig. 2. The database on topology of the terrain has been created in a global coordinate system, digitalizing the isolines, so each isoline is presented with a series of equations of second order curves passing through three neighboring points on it. The main central cross section fig. 2, should be

¹ Assistant Professor, IZIS-Skopje, Macedonia. Email: violeta@pluto.izis.ukim.edu.mk

² Professor, IZIS-Skopje, Macedonia. Email: violeta@pluto.izis.ukim.edu.mk

defined in its local coordinate system. The coordinates of any point that belongs to the plain model in respect to the global coordinate system "X_G-Z_G-Y_G" are defined by transformation of coordinates of the plain model on the local coordinate system "x_l-y_l-z_l" into the local coordinate system "X_L-Y_L-Z_L" whereat Y_{CL}=0, X_{CL} ≠ 0 and Z_{CL} = 0 if the absolute Z coordinates are used in definition of the plain model

$$\begin{Bmatrix} X_L \\ Y_L \\ Z_L \end{Bmatrix} = \begin{bmatrix} 0 & 1 & 0 \\ -1 & 0 & 0 \\ 0 & 0 & 1 \end{bmatrix} \begin{Bmatrix} x_l \\ y_l \\ z_l \end{Bmatrix} + \begin{Bmatrix} Y_{CL} \\ X_{CL} \\ Z_{CL} \end{Bmatrix} \quad (1)$$

and transformation of the coordinates from the local system "X_L-Z_L-Y_L" into the global system "X_G-Z_G-Y_G", whereat coordinate X_L = 0.

$$\begin{Bmatrix} X_G \\ Y_G \\ Z_G \end{Bmatrix} = \begin{bmatrix} C & -S & 0 \\ S & C & 0 \\ 0 & 0 & 1 \end{bmatrix} \begin{Bmatrix} X_L \\ Y_L \\ Z_L \end{Bmatrix} + \begin{Bmatrix} X_C \\ Y_C \\ Z_C \end{Bmatrix} \quad (2)$$

At each altitude, the coordinates of characteristic intersection points with the boundary lines of plain model are defined, fig. 2. Drawn through these points are straight lines parallel to the dam crest axis. So obtained in this way are the cross sections of the dam body with the terrain at each altitude. For definition of the 3D model adopted for the analysis we should select only the characteristic cross sections, otherwise we will have a considerably dense substructure and F.E. mesh, that will result in an increased value of matrix band. Fig. 3, provides a cumulative presentation of only selected horizontal cross sections that are used for definition of the 3D mathematical model presented in fig. 4. The program further performs automatic generation of F.E. mesh with required density. It also, automatically links the substructures. That results in a certain initial value of the matrix band. Elaborated is a subroutine for reducing the band by 20%. The adopted 3D mathematical model has a total number of substructures of 212, external substructures' nodes of 6250, internal substructures' nodes of 2122 and matrix band of 2200.

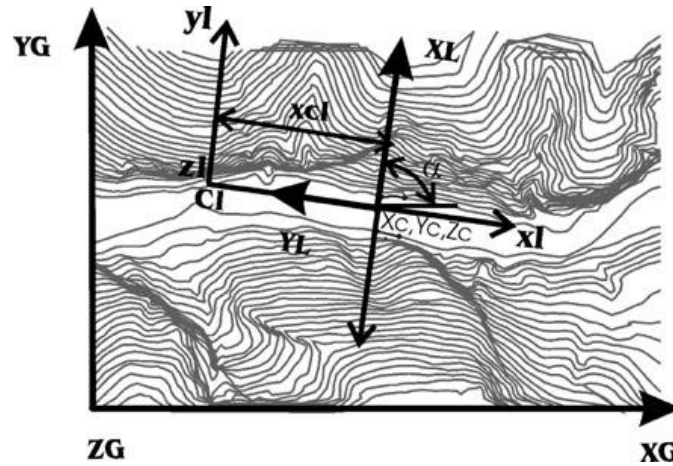


Fig. 1. Schematic presentation of the required position of dam body with indication of individual

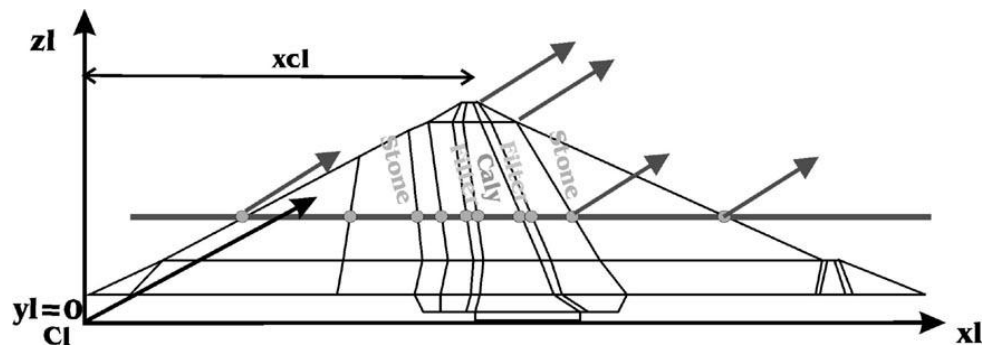


Fig. 2. Central cross-section with zones of presence of different materials

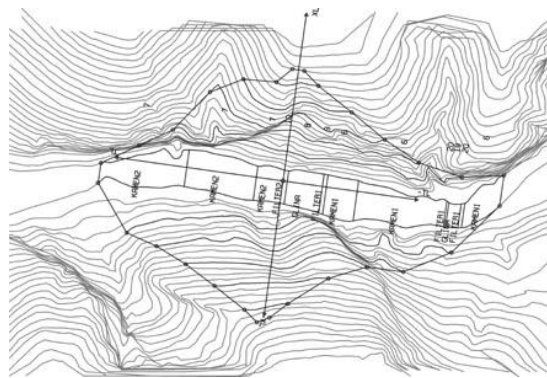


Fig. 3. Cumulative presentation of the selected levels used for generation of the model

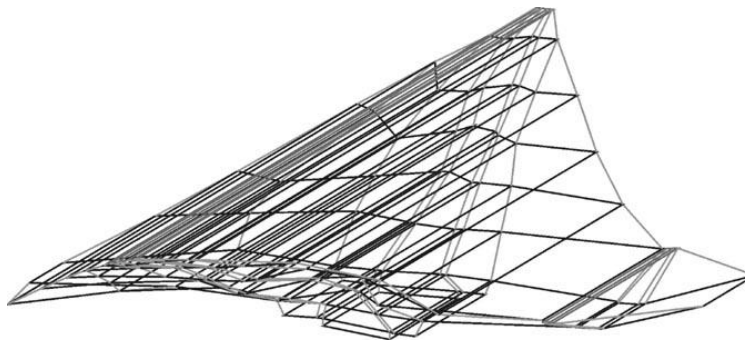


Fig. 4. 3D Mathematical model of substructures adopted for analysis

STATIONARY FILTRATION REGIME AND PORE PRESSURES

While analyzing the stress and strain state of dams constructed of local materials, the pore pressures in the porous media have a considerable influence, since the shear strength is directly dependent on the effective stress values. The pore pressures in the porous media are variable in the course of the serviceability of the structure. However, in conditions of stationary filtration regime, they are independent of the stresses and unchangeable until the conditions under which the stationary filtration is established are changed. The main equation for solving the potential function in 3D stationary filtration conditions is the Laplace's differential equation.

$$k_{xx} \frac{\partial^2 W}{\partial x^2} + k_{yy} \frac{\partial^2 W}{\partial y^2} + k_{zz} \frac{\partial^2 W}{\partial z^2} = 0 \quad (3)$$

k_{xx}, k_{yy}, k_{zz} – permeability coefficients for orthotropic medium

$W(x, y, z)$ – potential function

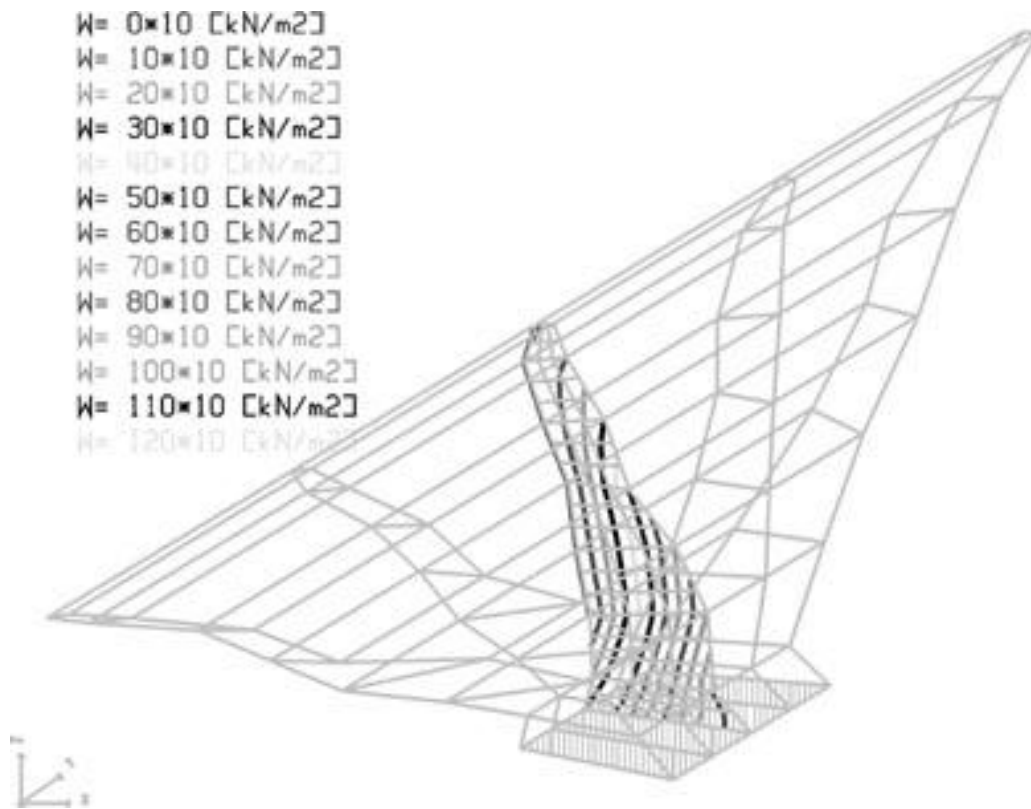


Fig. 5. Equilines of pore pressure in the central cross section of the clayey core

The numerical technique follows the finite element technique. The mathematical model for solving the 3D stationary filtration is obtained automatically from the 3D mathematical model of the dam, by extraction of substructures in which there are porous media. The compatibility of both mathematical models enables

determination of effective stresses by superposing the obtained total stresses from the static analysis with the pore pressures. The pore pressure at each point of the clayey core is obtained as a difference between the potential and the geodetic height of the point in respect to the selected referent plane. The pore pressure drops starting from the upstream slope toward the downstream slope of the core and is increased along the core depth, fig. 5. The vector of the gradient of the potential field is normal to the equipotential surfaces, so the lines of the flow, i.e., the filtration speed are normal to the equipotential surfaces, fig.6. The greatest filtration speed takes place at the transition of the filtered water from the clay into the filters on the downstream side, at the height of the downstream water.

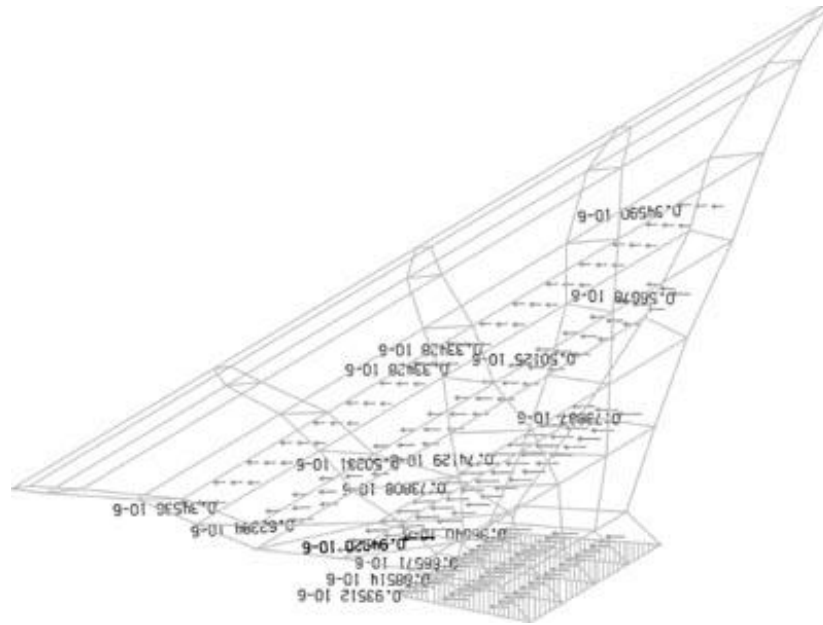


Fig.6. Filtration velocities in selected cross sections of the clayey core (m/sec)

STRESS - STRAIN STATE DUE TO THE DEAD WEIGHT

The determination of the stress-strain state in the dam, by application of the mathematical model presented in fig. 4, has been done by using the single lift analysis. The soil materials incorporated into the dam are treated as linearly elastic and non-linear elasto-plastic material media according to the Mohr-Coulomb's criterion. The total maximum expected deformation of the crest is $U = 4.4$ m when treating the incorporated soil materials as ideally elasto-plastic. Part of this total deformation represents an elastic deformation which takes place in the course of building of the layers during incremental construction and it amounts to $U = 3.7$ m. The plastic deformation is 16-17% of the total one. The development of deformations and stress state in the dam body is a result from the geometrical characteristics of the structure dictated by the shape of the canyon. Due to the steep contact between the dam and the rock massif, tensile stresses take place on both banks, in the upper third of the dam, in the zones immediately next to the contact with the rock. The intensity of these tensile stresses decreases from the contact zone toward the inner part. Fig. 7 and fig. 8 show the state of deformations along with the zones of occurrence of tensile strains in one longitudinal section through the dam body. Presented in fig. 9 and fig. 10 is the stress state, due to the dead weight, in the case of treating the material medium as linearly elastic and elasto-plastic. It can be seen that there is a drastic difference in the stress state obtained on the basis of these two analyses. In the linear analysis, there is a wide zone of occurrence of tensile stresses near the dam-rock contact. In the non-linear analysis, tensile stresses occur only in the upper third of the height of

the clayey core. These tensile stresses are lower than the allowable ones and do not induce cracks in the clay. During the non-linear analysis, tensile stresses are absent in the crushed stone and filtering layers because they cannot be sustained by the non-coherent material media. Excessive tensile stresses in non-coherent material media cause tensile strains and crack occurrence. Fig. 11a, shows the principal stresses σ_1 [kN/m²] in one part of the longitudinal section $x_l=0$ m, according to the analysis with non-linear behaviour of the spring elements, placed in the contact between dam and the rock, and in the case of assumed linear material behaviour of the dam body. If these stresses are compared to the stresses in the same section obtained from the linear analysis, in conditions of total fixation of the model at the support, fig. 11b, it can be concluded that there is a decrease of intensity of tensile stresses down to 20%, in the case when motion at the contact with the rock is allowed. So the appearance of tensile stresses in the zones close to the rock do not result only from the bending deformation effect but also result from the effect of the supporting conditions (extent of fixation in the model).

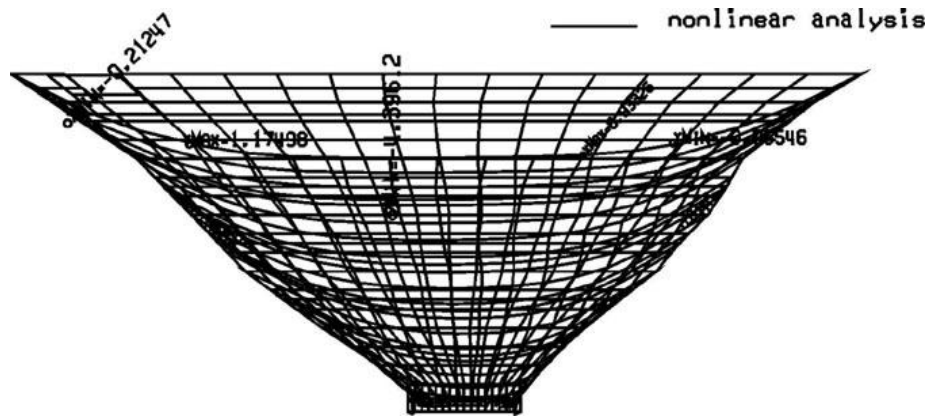


Fig.7. Deformation shape in (m) for longitudinal section $x_l=0$ with marked cracked zones

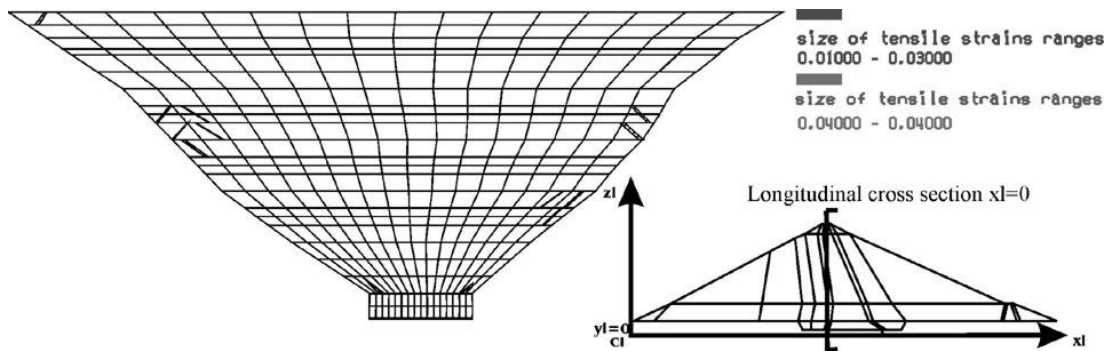


Fig.8. Developed cracks in longitudinal section $x_l=0$ with position of the section

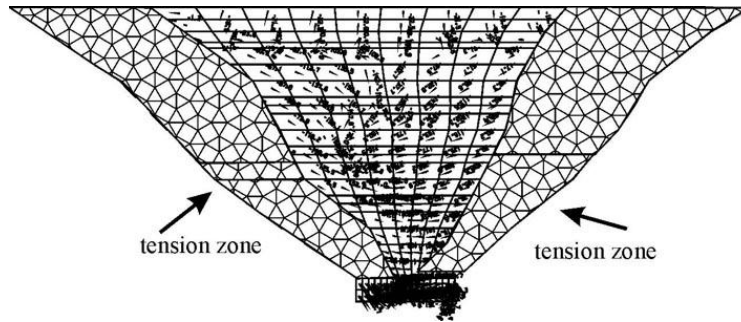


Fig. 9. Principal stresses σ_1 in longitudinal section $x_l=0$. (due to the linear analysis)

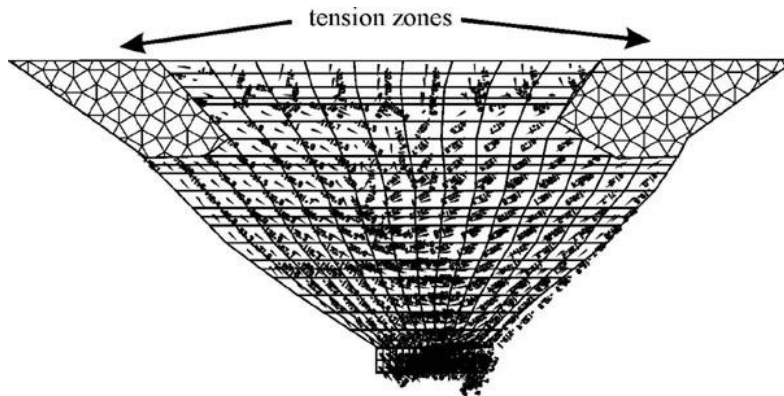


Fig. 10. Principal stresses σ_1 in longitudinal section $x_l=0$. (due to the non-linear analysis)

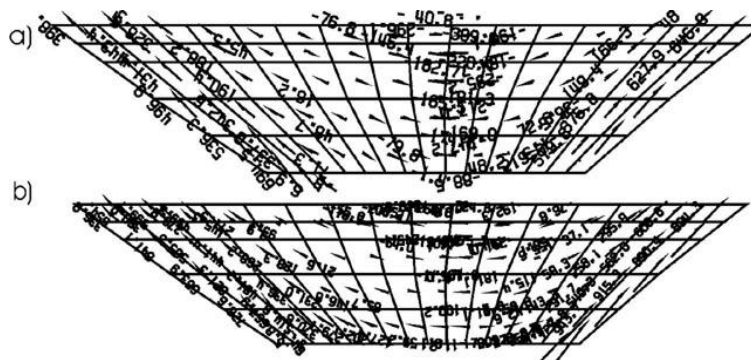


Fig. 11. Principal stresses σ_1 : a) analysis with contact elements b) analysis with fixed model

DYNAMIC RESPONSE OF THE DAM

Used for the performance of the dynamic analysis for determination of the dynamic response of the dam, were the methods of modal analysis as well as direct "step by step" linear integration (linear analysis) and direct "step by step" linear integration (non-linear analysis) with incorporated law on non-linear behaviour of soil media. Comparing the results obtained by modal analysis and linear "step by step" direct integration, both methods have been verified, first of all, because the computer program for "step by step" linear direct integration (linear analysis) serves as a basis for preparation of the computer program for non-linear analysis.

Within the frames of each finite element, the iterative procedure "Load Transfer Method" is applied, whereat elimination of the vector of excessive stresses, i.e., corresponding residual forces defined in accordance with the Mohr-Coulomb's failure criterion is done iteratively.

The first step in this method is solving the equation of dynamic equilibrium within the frames of each "i"-th time step and each iteration:

$$M ** \Delta \ddot{U}_i + C ** \Delta \dot{U}_i + K ** \Delta U_i = \Delta P_i ** \quad (4)$$

Applying the substructure concept, the differential equation of motion refers only to the external points of the mathematical model. Defined in that way are the incremental vectors of displacement, velocity and acceleration at the external points of the system. The dynamic response at the end of each time step is defined by summing up the dynamic response from the beginning of the time step and the effect from the iterations performed in it.

$$U_n = U_0 + \sum_{i=1}^n \Delta U_i \quad \dot{U}_n = \dot{U}_0 + \sum_{i=1}^n \Delta \dot{U}_i \quad \ddot{U}_n = \ddot{U}_0 + \sum_{i=1}^n \Delta \ddot{U}_i \quad n=1, iter \quad (5)$$

where:

- $iter$ - number of iterations within the frames of each time step;
- $U_0, \dot{U}_0, \ddot{U}_0$ - initial vectors of displacement, velocity and acceleration;
- $\Delta U_0, \Delta \dot{U}_0, \Delta \ddot{U}_0$ - incremental values of vectors of displacements, velocity and acceleration.

Using the incremental displacement vector, defined within each iteration is the vector of incremental strains and the corresponding vector of incremental stresses for each finite element. Herewith, the vector of incremental displacements of each finite element is defined by superposing of part of the vectors of incremental displacements for the external and the internal points of the finite element. The incremental vector of displacements of the inner points is obtained using the Guyan's transformation. For each finite element, the total vector of strains and stresses at the end of each iteration is defined as follows:

$$\varepsilon = \varepsilon_0 + \sum_{i=1}^n \Delta \varepsilon_i \quad \sigma = \sigma_0 + \sum_{i=1}^n \Delta \sigma_i \quad n=1, iter \quad (6)$$

where:

$iter$ - number of iterations within the frames of each time step;
 ϵ_0, σ_0 - initial vectors of strains and stresses;
 $\Delta\epsilon_0, \Delta\sigma_0$ - incremental vectors of strains and stresses.

At the end of each iteration, the stress state is reviewed for each finite element. Selected are only those finite elements for which the stress state is in the plasticity zone. Defined for these finite elements are the excessive stresses as a difference between the manifested and the ultimate stresses. Determined for such defined excessive stresses are the corresponding residual forces as follows:

$$\{f_{rez}^e\} = - \int_V [B]^T \{\Delta\sigma\}_e dv \quad (7)$$

Solving again the incremental differential equation of dynamic equilibrium only by consideration of the effect of the defined residual forces from the previous iteration, the new vectors of incremental displacements, strains and stresses are obtained in the next iteration.

Since the residual forces are applied on a system with unchanged stiffness matrix, the excessive stresses exist at each iteration but their intensities are decreased with the increase in the number of iterations, i.e., the iterative process converges. Successive iterations are done until the excessive stresses and the corresponding residual forces are higher than the tolerance of the iterative procedure.

The damping matrix, in explicit form, according to the *Rayleigh's* damping concept, is defined as follows:

$$[C] = \alpha[M] + \beta[K] \quad (8)$$

$$\alpha = \frac{2\omega_1\omega_2^2\xi_1 - 2\omega_2\omega_1^2\xi_2}{\omega_2^2 - \omega_1^2} \quad \beta = \frac{2\omega_2\xi_2 - 2\omega_1\xi_1}{\omega_2^2 - \omega_1^2} \quad (9)$$

For the purpose of defining coefficients α and β as competent coefficients for the energy dissipation, the first two mode shapes of natural vibrations with frequencies of $\omega_1=4.48$ rad/sec and $\omega_2=6.28$ rad/sec and modal dampings of $\xi_1=10\%$ and $\xi_2=15\%$ have been adopted.

Dynamic analysis has been performed for the effect of harmonic excitation with frequency of $\omega_0=5.2$ rad/sec, peak acceleration $A_0=0.3g$ and time duration of $T=20$ sec. The harmonic excitation has been applied only in the direction of the global X-axis of the system. The time step of direct integration is $\Delta t=0.02$ sec. Such a selected harmonic excitation whose frequency is close to the first fundamental mode of natural vibrations of the system has a large, i.e., dominant dynamic factor of participation in the system response. From the same reasons, the dynamic factor of participation of the remaining frequencies shall be lower, which is confirmed by the fact that the responses obtained by the modal analysis in which only the first mode of the system is included and the response obtained by direct integration (linear analysis), point to good correlation, particularly referring the response in the global X-axis.

In the case when non-linear analysis is applied, according to the Mohr-Coulomb's criterion, the manifested maximum shear strength of the finite elements that are in the plasticity zone is reduced down to the level of the ultimate shear stress, so that the mobilized strength acquires a unit value. It can be concluded that the mobilized strength in the case of non-linear analysis shall have a value equal to unity. The stability of the finite elements that have exerted a plastic behaviour should be judged on the basis of the manifested

plastic deformations in the domain of such finite elements. The defined safety coefficient against sliding, gives an information about the relationship between the passive forces sustaining the motion and the active forces that tend to cause motion of certain potential shear planes in a certain zone of the dam. The safety coefficient against sliding represents an average evaluation of the stability of a certain potential shear surface and is defined as follows:

$$F_s = \frac{\int_A (C + (\sigma_n - u) \tan \phi) dA}{\int_A \tau dA} \quad (10)$$

The following figures in the text, are obtained from the dynamic analysis of the dam using prepared computer program package that is written for WINDOWS operative system by use of FORTRAN 90, DIGITAL VISUAL FORTRAN compiler and library for graphic support PLOT88 for WINDOWS.

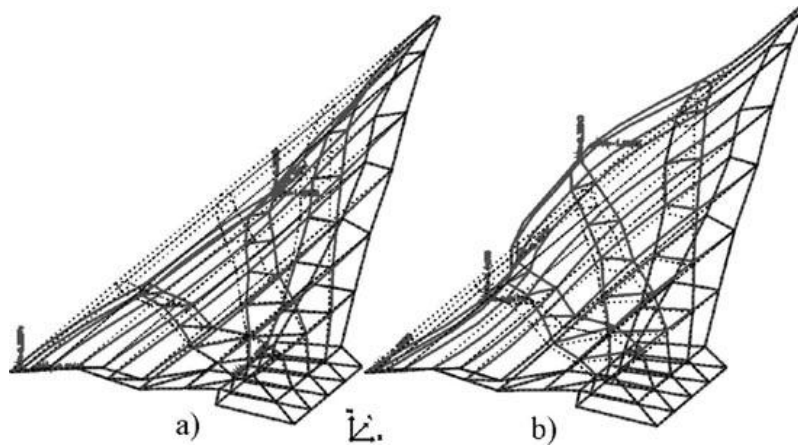


Fig.12. a) First mode shape T=1.4 sec b) Second mode shape T=1.0 sec

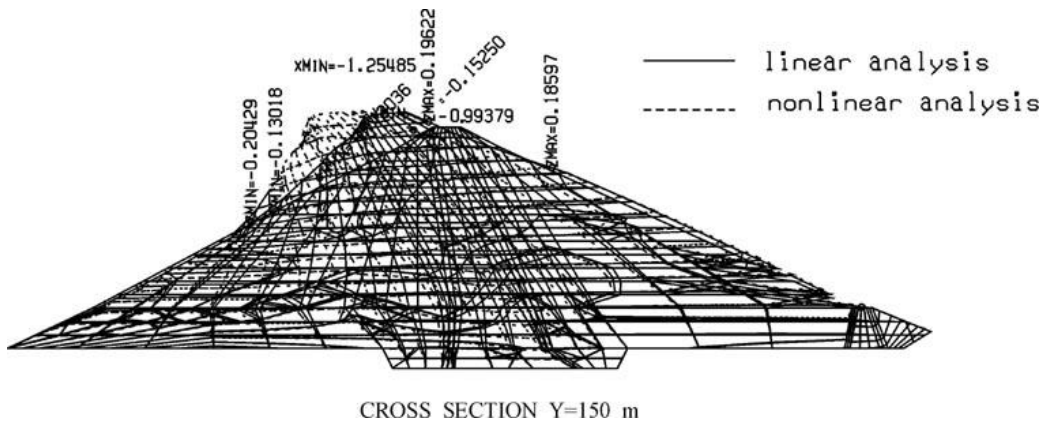


Fig. 13. Snapshot of deformations in time T=2.0 sec

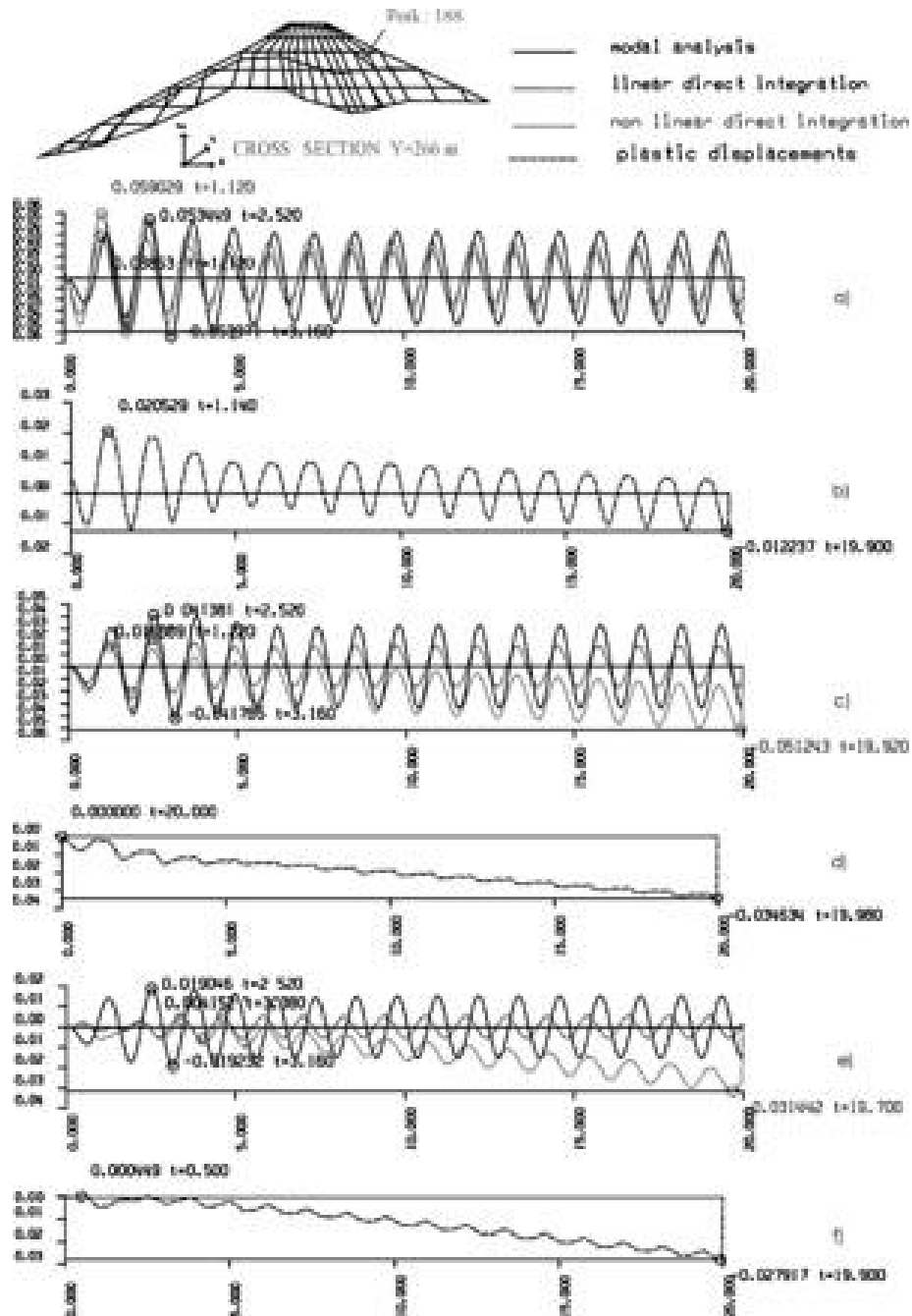
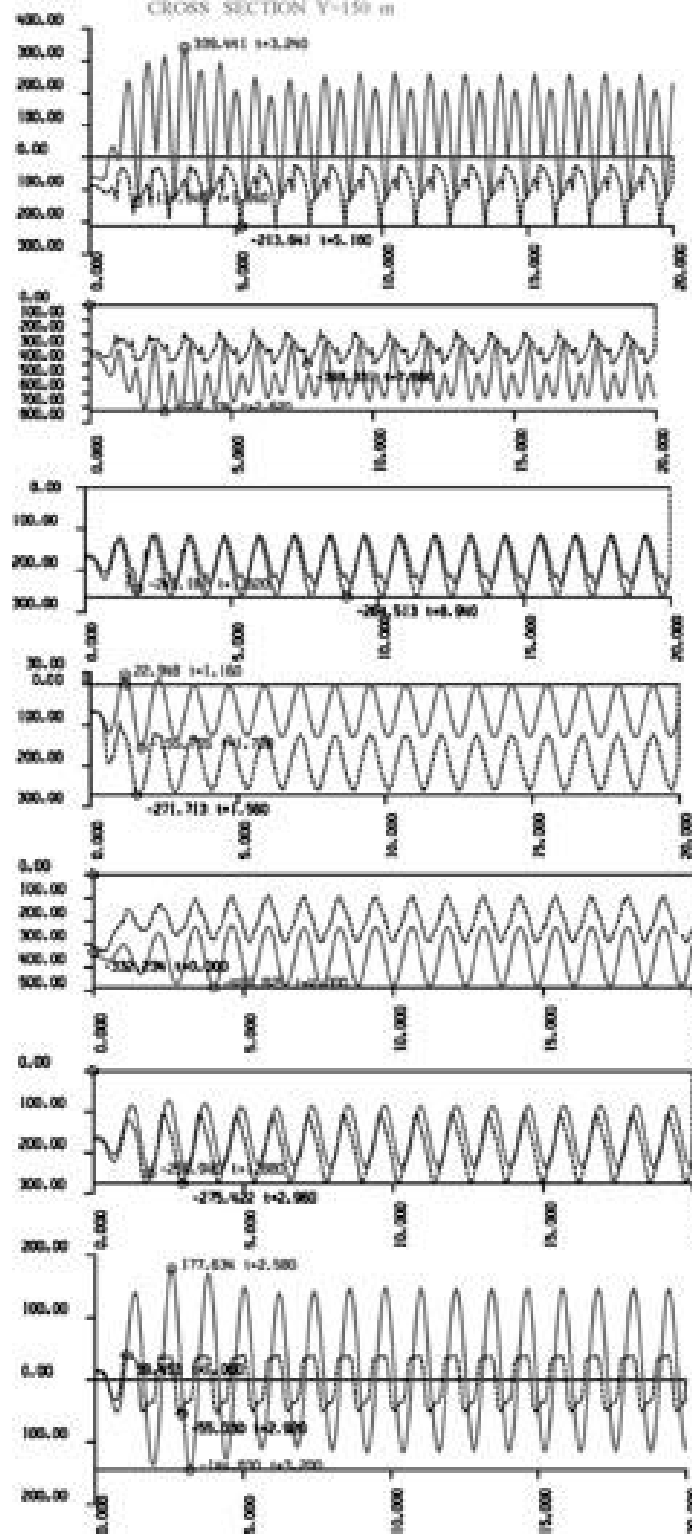


Fig. 14. Time histories of relative displacements in (m), (a) X-direction, (c) Y-direction, (e) Z-direction and (b) time histories of plastic deformations in X-direction, (d) Y-direction and (f) Z-direction



a)

b)

c)

d)

e)

f)

g)

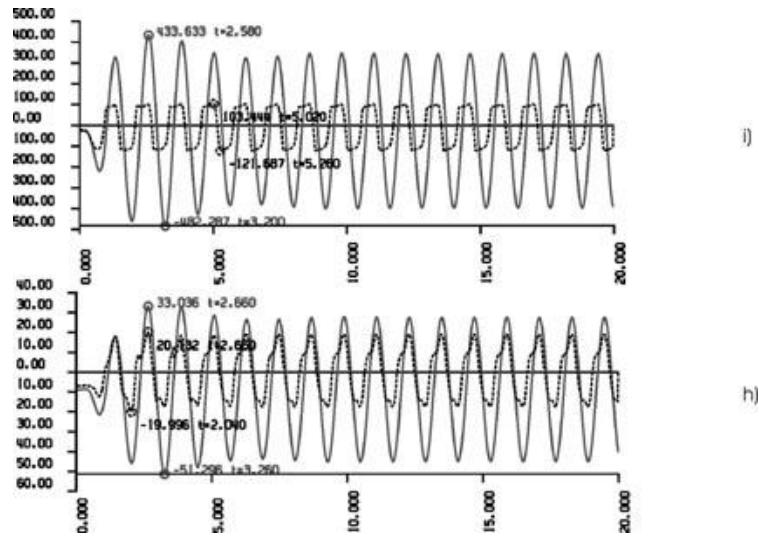


Fig. 15. Time histories of stresses [kN/m²] for the selected F.E due to harmonic excitation
a) principal stress σ_1 , b) principal stress σ_2 , c) principal stress σ_3 , d) component stress σ_x , e) component stress σ_y , f) component stress σ_z , g) component stress τ_{xy} , i) component stress τ_{xz} , h) component stress τ_{yz}

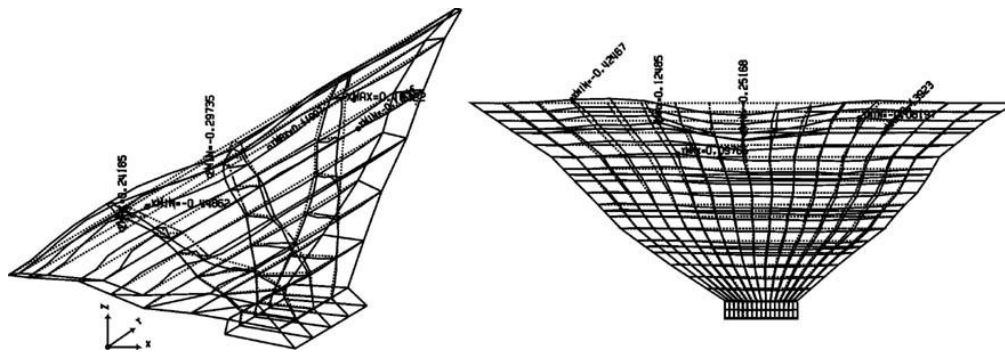


Fig. 16 Plastic deformations of the clayey core and in longitudinal section $x_l=0$

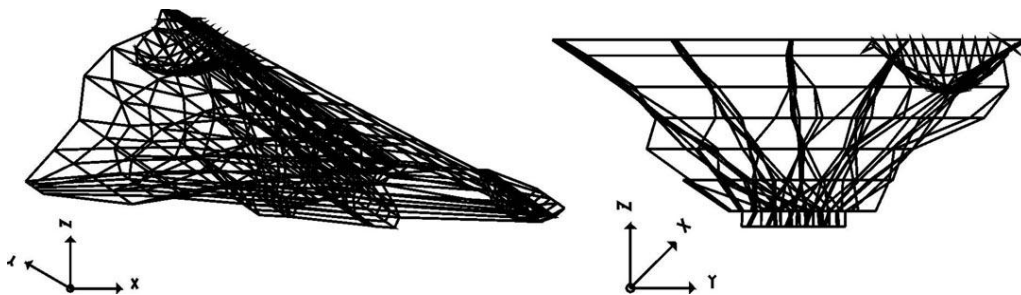


Fig. 17. Position of the potential sliding surface (shell) in the dam

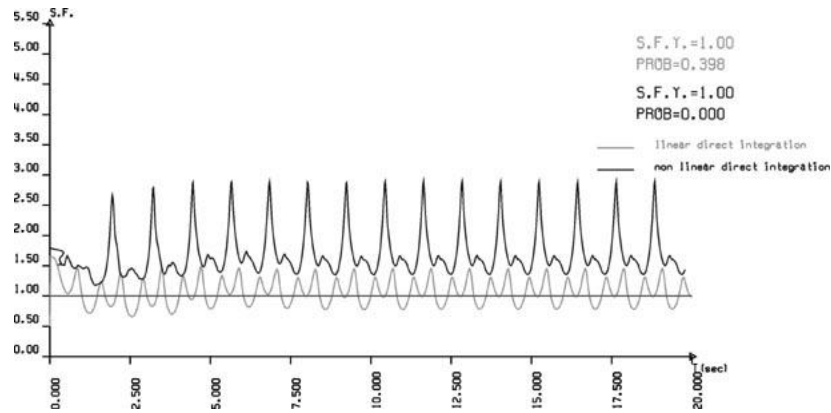


Fig. 18. Time history of safety coefficient against sliding

CONCLUSIONS

Geometrical shape of the canyon and the structure have dominant effect upon the stress-strain state whereby automatic generation and application of a *3D* mathematical model is necessary. There is a drastic difference in deformations and stress obtained on the basis of the performed linear and non-linear analysis. In the linear analysis, there is a wide zone of occurrence of tensile stresses in the vicinity of the dam-rock contact. In the non-linear analysis, the tensile stresses occur only in the upper third of the clayey core height. Using contact elements at the base of the model it is possible to model the degree of fixation in the support and eliminate the tensile stresses that result from unrealistic modeling of the supporting conditions, usually supporting conditions of total fixation. Based on the residual plastic deformations, it may be concluded that settlement of the dam takes place as a result of the non-linear dynamic response. The stress state in the deep zones of the dam is in the range of pure pressure, with greater intensity of spherical stresses, which results in a slightly expressed non-linearity. When reaching the state of ultimate plastic equilibrium, the active shear forces are under control at the expense of which are developed additional plastic deformations whose intensities are competent for the evaluation of the stability of the integral dam.

REFERENCES

1. Pastor, M., Zienkiewicz, O.C., Chan, A.H.C., General plasticity and modeling of soil behaviour, *IJNAMG*, Vol. 14, 151-190, 1990.
2. Chen, W.F., Baladi, G.Y., Soil plasticity: Theory and implementation, Elsevier Science Publishers, 1985
3. Owen, D.R.J., Hinton, E., Finite elements in plasticity: theory and practice, Pineridge Press, Swansea, U.K., 1980.